Published on 12 June 2015. Downloaded by Changchun Institute of Optics, Fine Mechanics and Physics, CAS on 29/05/2016 15:01:57.

RSC Advances

ROYAL SOCIETY OF CHEMISTRY

PAPER

View Article Online
View Journal | View Issue

Cite this: RSC Adv., 2015, 5, 54947

Effective intensity distributions used for direct laser interference exposure

Jia Xu,[ab] Zuobin Wang,*[bc] Ziang Zhang,[b] Dapeng Wang[bc] and Zhankun Weng[b]

Received 29th April 2015
Accepted 12th June 2015

DOI: 10.1039/c5ra06504f

www.rsc.org/advances

This paper presents a method to obtain periodic structures with different feature shapes using direct laser interference lithography. In the method, the desired structures are produced by controlling the effective intensity distributions of interference patterns during the exposure process. The effective intensity distributions are adjusted by changing the exposure beam intensity based on the material modification thresholds. In the simulations and experiments, different exposure intensities were used to study the interactions between the effective intensity distributions and the materials, and direct four- and six-beam laser interference lithography systems were set up to pattern silicon wafers. The shapes and sizes of the fabricated surface structures changed with the effective intensities. The experimental results are in accordance with the theoretical models and simulations.

Laser interference lithography is a patterning technology for the fabrication of periodic and quasi-periodic micro- and nano-structures.[1–3] It has a much larger exposure area and deeper exposure field than other lithography technologies, and it has the advantages of low cost and high throughput in fabricating gratings, periodic structured templates, 3D photonic crystals, micro- and nano-photonic devices and photoelectric sensors.[4–6]

The process of traditional laser interference lithography utilizes the interference patterns generated by two or more coherent laser beams to obtain the desired surface structures.[7,8] The technology was developed into a multi-step process.[9,10] A photoresist is used as the sensitive material covered on the sample surface by spin-coating, and then the interference patterns are transferred to the material surface after exposure, development and etching.[11–14] With the development of direct laser interference lithography, the interference patterns based on the high-power laser can be written into the material surface directly without the photoresist and masks to form periodic fringe and dot arrays. It has the advantages of simplicity, high efficiency and 3D patterning compared with traditional interference lithography.[15–19] In this case, the effective intensity distributions of the interference patterns can be used to obtain different shapes of surface structures in an interference system.

In the direct laser interference lithography system, it is assumed that the lithography threshold of the sample is P, and the intensity of the interference pattern is P_s. The effective intensity distribution used to directly modify the sample surface P_e can be expressed as $P_e = P_s - P(0 < P_e < P_s)$. The effective intensity distribution is significant for a direct laser interference lithography system, as it is related to the formation of the shape of the surface structures when the wavelength, beam numbers, azimuth angles, incidence angles and polarization directions are selected. Different surface patterns can be obtained using different effective intensity distributions, and the effective intensity distributions can be controlled by adjusting the exposure beam intensity over the material modification threshold.

In this work, we describe theoretical models and simulations of direct four- and six-beam laser interference, and use the effective intensity distribution of the interference patterns to modify the silicon wafer surface. The desired periodic structures were fabricated directly on the material surface by appropriate selection of an interference intensity distribution over the thresholds. The morphology of the exposure structures is characterized using SEM, and the experimental results show that the effective intensity distribution of the interference patterns can be used to form periodic structures with different sizes and shapes in the direct laser interference lithography system.

Theoretical analysis and simulations

The general form of N-beam laser interference can be described as the superposition of the electric field vectors of N coherent beams. The electric field vector of the n-th beam can be expressed as[20]

$$\vec{E}_n = A_n \vec{p}_n \cos(\vec{k}_n \cdot \vec{r}_n - \omega t + \varphi_n) \quad (1)$$

[a]Changchun Institute of Optics, Fine Mechanics and Physics, Chinese Academy of Sciences, Changchun 130033, China

[b]CNM & JR3CN, Changchun University of Science and Technology, Changchun 130022, China. E-mail: wangz@cust.edu.cn

[c]JR3CN & IRAC, University of Bedfordshire, Luton LU1 3JU, UK

View Article Online

Published on 12 June 2015. Downloaded by Changchun Institute of Optics, Fine Mechanics and Physics, CAS on 29/05/2016 15:01:57.

where A_n is the amplitude, $\vec{p}_n$ is the unit polarization vector, $\vec{k}_n$ is the vector in the propagation direction, $\vec{r}_n$ is the position vector, ω is the frequency and φ_n is the initial phase.

For eqn (1), $\vec{r}_n$, $\vec{p}_n$ and $\vec{k}_n$ can be expressed as

$$\vec{r}_n = x\cdot\vec{a} + y\cdot\vec{b} + z\cdot\vec{c} \tag{2}$$

$$\vec{k}_n = k(\sin\theta_n\cdot\cos\phi_n\cdot\vec{a} + \sin\theta_n\sin\phi_n\vec{b} - \cos\theta_n\cdot\vec{c}) \tag{3}$$

$$\vec{p}_n = -(\cos\theta_n\cdot\cos\phi_n\cdot\cos\psi_n - \sin\theta_n\sin\psi_n)\vec{a} - (\cos\theta_n\cdot\sin\phi_n\cdot\cos\psi_n + \cos\theta_n\sin\psi_n)\vec{b} - (\sin\phi_n\cdot\cos\psi_n)\vec{c} \tag{4}$$

where $k = 2\pi/\lambda$, $\vec{a}$ is the vector in the x-axis direction, $\vec{b}$ is the vector in the y-axis direction, $\vec{c}$ is the vector in the z-axis direction, λ is the wavelength, θ_n is the incidence angle, ϕ_n is the azimuth angle and ψ_n is the polarization angle. For the N-beam interference field, the intensity distribution can be expressed as

$$I(r) = \sum_{n=1}^{N}\sum_{m=1}^{N} A_n\vec{p}_n\cdot A_m\vec{p}_m\cdot e^{\left[i\left(\vec{k}_n-\vec{k}_m\right)\vec{r}+\phi_n-\phi_m\right]} \tag{5}$$

In the experiments, systems of four- and six-beam laser interference lithography are used to obtain the desired interference patterns by fixing the number of beams to four and six. Four-beam laser interference can generate patterns with an array of dots or holes, and six-beam laser interference can generate modulated patterns.

Direct four-beam interference

The illustration of a direct four-beam interference setup is shown in Fig. 1. For the direct four-beam interference, the laser source is divided into four beams with azimuth angles of $\varphi_1 = 0°$, $\varphi_2 = 90°$, $\varphi_3 = 180°$ and $\varphi_4 = 270°$, and incidence angles of $\theta_1 = \theta_2 = \theta_3 = \theta_4 = \theta$. It is assumed that the amplitudes of the beams are identical. The intensity of the interference is expressed as

$$I_{\text{Four-beam}} = 2A^2\left\{\begin{array}{l} 2+\cos(2kx\sin\theta)+\cos(2ky\sin\theta)+ \\ 2\cos[k(x-y)\sin\theta]+2\cos[k(x+y)\sin\theta] \end{array}\right\} \tag{6}$$

To study the interaction between the effective intensity distribution and the threshold of the material, a simulation of direct four-beam laser interference exposure was performed to obtain the interference patterns.[21–24] In the simulation, interference patterns with different effective intensity distribution shapes were obtained, as shown in Fig. 2. With the reduction of the exposure beam intensity over the material modification thresholds, the shape of the periodic patterns changed gradually during the direct interference exposure, such as forming periodic hole-arrays, periodic grid-arrays and periodic elliptical dot-arrays.

Direct six-beam interference exposures

Moth-eye structures have the unique feature of a high absorption of the incidence light due to the dual structure distribution on the surface.[25–28] To obtain structures similar to moth-eyes, the effective intensity distribution used for direct six-beam laser interference is designed to fabricate moth-eye-like dual structures.

Compared with six azimuth angles, a configuration of four azimuth angles has the advantage of good controllability regarding the pattern structures in the direct six-beam interference lithography system. As shown in Fig. 3, the six incidence beams follow a configuration with azimuth angles of $\varphi_1 = 0°$, $\varphi_3 = \varphi_5 = 180°$, $\varphi_2 = 270°$ and $\varphi_2 = \varphi_4 = 90°$. The incidence angles of the six beams can be set as $\theta_1 = \theta_2 = \theta_3 = \theta_4 = \theta$ and $\theta_5 = \theta_6 = \theta + \delta$. It is assumed that the amplitudes of the six beams are identical and the initial phases are zero. According to eqn (5), the intensity distribution of the six-beam interference field can be calculated by

$$I = 2A^2\left\{\begin{array}{l} 3-\cos(2k\sin\theta\cdot x)+\cos\left\{\begin{array}{l}[\sin\theta-\sin(\theta+\delta)]x \\ -[\cos\theta-\cos(\theta+\delta)]z\end{array}\right\} \\ -\cos\left\{\begin{array}{l}[\sin\theta+\sin(\theta+\delta)]x+ \\ [\cos\theta-\cos(\theta+\delta)]z\end{array}\right\} \\ -\cos(2k\sin\theta\cdot y)+\cos\left\{\begin{array}{l}[\sin\theta-\sin(\theta+\delta)]y \\ -[\cos\theta-\cos(\theta+\delta)]z\end{array}\right\} \\ -\cos\left\{\begin{array}{l}[\sin\theta+\sin(\theta+\delta)]y+ \\ [\cos\theta-\cos(\theta+\delta)]z\end{array}\right\} \end{array}\right\} \tag{7}$$

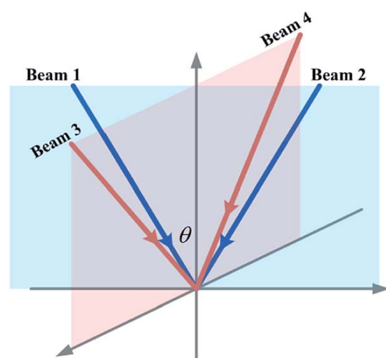

Fig. 1 Direct four-beam interference configuration: beam 1 and beam 2 are in the same incidence plane which is orthogonal to the plane of beam 3 and beam 4.

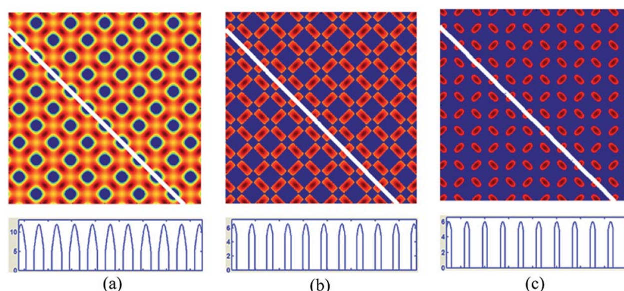

Fig. 2 Effective intensity distributions used for the direct four-beam interference with reduced exposure beam intensities: (a) periodic hole-arrays; (b) periodic grid-arrays; (c) periodic elliptical dot-arrays.

 This journal is © The Royal Society of Chemistry 2015

Published on 12 June 2015. Downloaded by Changchun Institute of Optics, Fine Mechanics and Physics, CAS on 29/05/2016 15:01:57.

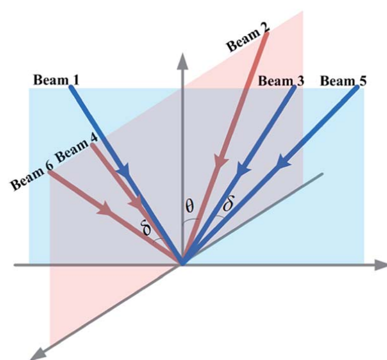

Fig. 3 Direct six-beam interference configuration: beam 1, beam 3 and beam 5 are in the same incidence plane which is orthogonal to the plane of beam 2, beam 4 and beam 6.

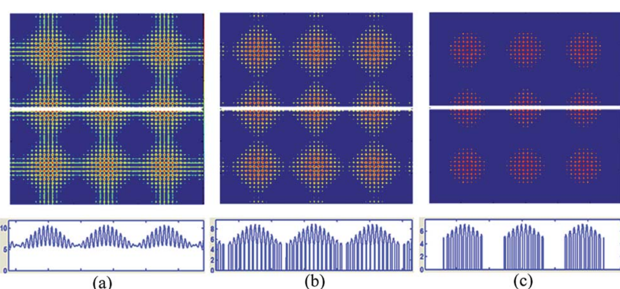

Fig. 4 Effective intensity distributions used for the formation of dual structures in direct six-beam interference.

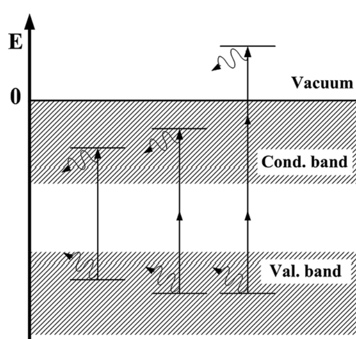

Fig. 5 Primary electronic excitation in semiconductors by absorption of photons.

As shown in Fig. 4(a)–(c), dual structures are obtained with the reduction of the effective intensity distributions during the direct six-beam interference simulations. The desired periodic dot structures can be fabricated by appropriate selection of an interference intensity distribution over the thresholds.

Experiments

The interaction process between the intensity distribution of the interference pattern and the silicon surface is the excitation of the electrons from the equilibrium states to the excited states

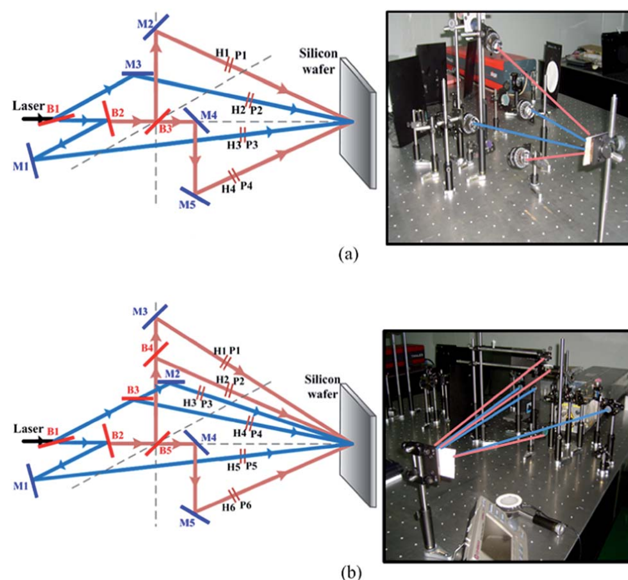

Fig. 6 Schematic and real set-ups for (a) four-beam laser interference; (b) six-beam laser interference. M1–M5 are the high-reflective mirrors, B1–B5 are the beam-splitters, H1–H6 are the half-wave plates and P1–P6 are the polarizers.

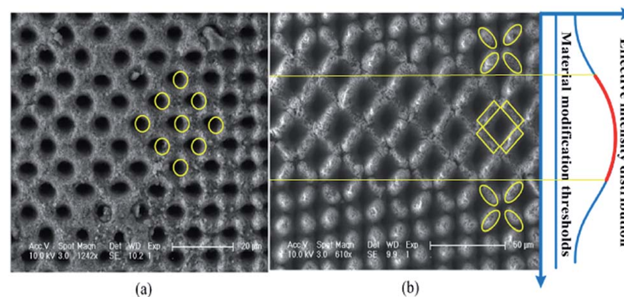

Fig. 7 SEM micrographs of the periodic structures fabricated by the direct four-beam interference with a reduced exposure beam intensity over the material modification thresholds: (a) periodic hole-arrays; (b) periodic grid-arrays and periodic elliptical dot-arrays.

by the absorption of photons, as shown schematically in Fig. 5. In the exposure process of direct laser interference lithography, the electrons are excited from the valence band to the conduction band by the absorption of photons. It is known that for a given interference pattern the effective intensity distribution induces the subsequent processes including melting, boiling and ablation of silicon. In this work, the smallest size that we have obtained using this method is about 20 nm.

In the experiments, four- and six-beam interference lithography systems were set up. As shown in Fig. 6, a pulsed Nd:YAG laser with a wavelength of 1064 nm, laser fluence of about 1800 mJ cm^{-2}, exposure frequency of 10 Hz, beam diameter of 9 mm and pulse duration of 6–8 ns was used as the system light source. The laser beam was split into four and six beams by beam splitters B1–B5. The incidence angle and azimuth angle of each beam were adjusted by controlling the positions of mirrors

Published on 12 June 2015. Downloaded by Changchun Institute of Optics, Fine Mechanics and Physics, CAS on 29/05/2016 15:01:57.

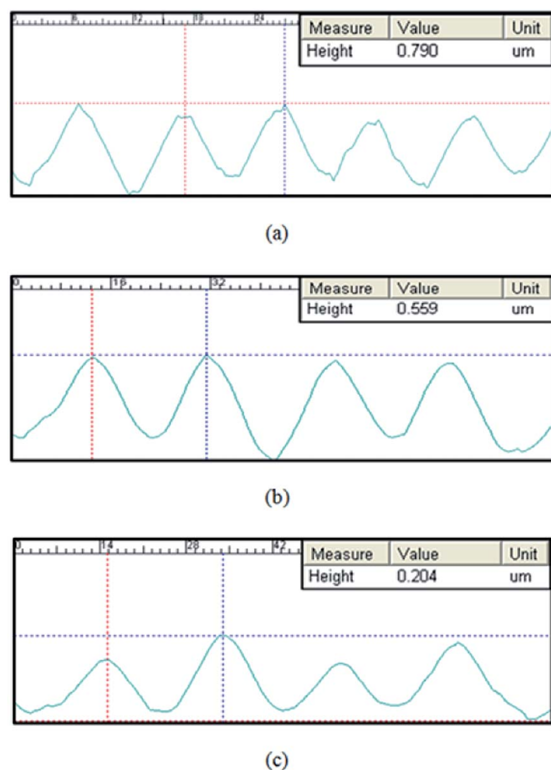

Fig. 8 Cross-sectional views of the periodic structures fabricated by the direct four-beam interference with reduced exposure beam intensity: (a) periodic hole-arrays; (b) and (c) periodic grid-arrays and periodic elliptical dot-arrays.

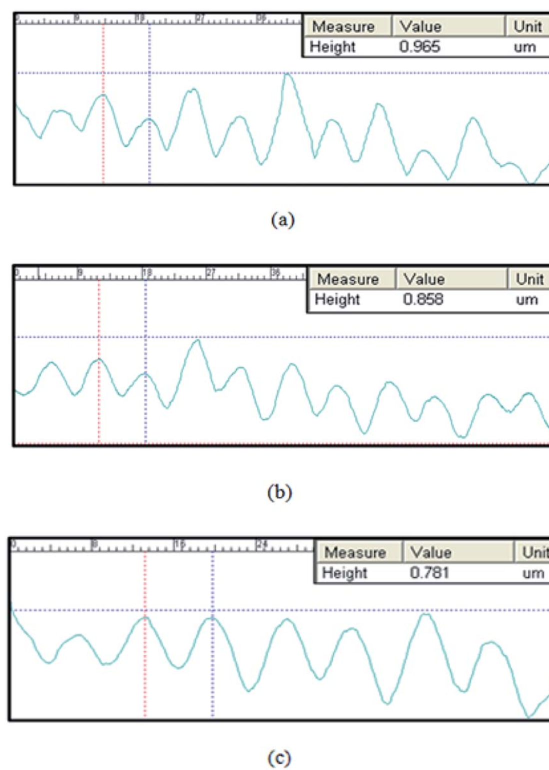

Fig. 10 Cross-sectional views of the dual structures fabricated by the direct six-beam interference with different exposure intensities: (a) pulse energy density of 30 mJ cm^{-2}; (b) pulse energy density of 22 mJ cm^{-2}; (c) pulse energy density of 15 mJ cm^{-2}.

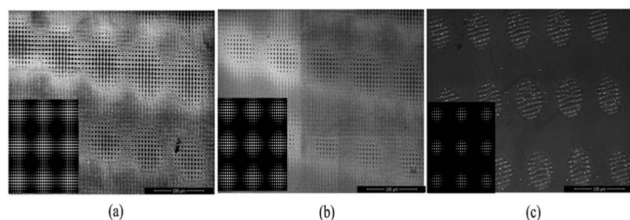

Fig. 9 SEM micrographs of the dual structures formed with different exposure intensities: (a) pulse energy density of 30 mJ cm^{-2}; (b) pulse energy density of 22 mJ cm^{-2}; (c) pulse energy density of 15 mJ cm^{-2}.

M1–M5. The half-wave plates H1–H6 and polarizers P1–P6 were used to select the polarization directions and exposure intensities for each beam before the beams interfere on the sample wafer surface. The samples used in the exposure were polished single crystal P-doped silicon wafers, and all the processes were carried out under clean-room conditions.

Results and discussion

In the experiment of direct four-beam interference lithography, the laser source was divided into four beams with azimuth angles of $\varphi_1 = 0°$, $\varphi_2 = 90°$, $\varphi_3 = 180°$ and $\varphi_4 = 270°$. The four coherent beams were incident on the sample surface with identical incidence angles of $\theta = 5°$. The laser fluence was about 640 mJ cm^{-2} for 60 s. Because of the non-flat intensity distribution of the laser spot, structures based on the different effective intensity distributions were obtained from the centre to the edge of the spot. Fig. 7(a) and (b) show the SEM micrographs of the periodic structures from the direct four-beam interference with a reduced exposure beam intensity over the material modification thresholds. As shown in Fig. 7(a), periodic hole-arrays were formed due to the stronger power of the spot centre. Fig. 7(b) shows the periodic grid-arrays and elliptical dot-arrays formed in the area located on the spot edge. Fig. 8(a) and (b) show cross-sectional views (Carl Zeiss Axio CSM 700 confocal microscope) of the periodic structures fabricated by the direct four-beam interference with a reduced exposure beam intensity over the material modification thresholds.

In the process of direct six-beam interference exposure, the laser beam was divided into six beams with azimuth angles of $\varphi_1 = 0°$, $\varphi_3 = \varphi_5 = 180°$, $\varphi_2 = 270°$ and $\varphi_2 = \varphi_4 = 90°$. The incidence angles of the six beams were set as $\theta_1 = \theta_2 = \theta_3 = \theta_4 = \theta = 7°$. Six half-wave plates and six polarizers were placed in pairs before the six interfering beams to obtain TE coherent beams and adjust the exposure intensities. Different exposure doses were used to determine the optimum dose for the desired patterns. In this case, the results were achieved with pulse energy densities of 30 mJ cm^{-2}, 22 mJ cm^{-2} and 15 mJ cm^{-2}, as shown in Fig. 9(a)–(c). The cross-sectional views of the periodic structures fabricated by the direct six-beam interference with different exposure intensities are shown in Fig. 10.

 This journal is © The Royal Society of Chemistry 2015

Published on 12 June 2015. Downloaded by Changchun Institute of Optics, Fine Mechanics and Physics, CAS on 29/05/2016 15:01:57.

Conclusion

In this work, a method to obtain periodic structures with different feature shapes has been presented and examined using direct laser interference lithography. The method features control of the effective intensity distributions used for the fabrication of periodic surface structures.

The effective intensity distributions can be controlled by changing the exposure intensity based on the material modification thresholds during the exposure process. The results of the simulations and experiments achieved by direct four- and six-beam laser interference have shown that the desired periodic structures can be fabricated directly on the silicon surface by appropriate selection of the effective intensity distribution of the interference patterns. There is good correspondence between the resulting structures and the theoretical models and simulations.

References

1 Q. Xie, M. H. Hong, H. L. Tan, G. X. Chen, L. P. Shi and T. C. Chong, *J. Alloys Compd.*, 2008, **449**, 261.
2 L. F. Johnson, G. W. Kammlott and K. A. Ingersoll, *Appl. Opt.*, 1978, **17**, 1165.
3 Z. Wang, J. Zhang, C. S. Peng and C. Tan, in *Proceedings of IEEE Conference on Mechatronics and Automation*, Institute of Electrical and Electronics Engineers, Harbin, 2007, pp. 434–439.
4 Y. F. Liu, J. Feng, Y. G. Bai, J. F. Song, Y. Jin, Q. D. Chen and H. B. Sun, *Opt. Lett.*, 2012, **37**, 124.
5 X. Zhang, J. Feng, J. Song, X. Li and H. Sun, *Opt. Lett.*, 2011, **36**, 3915.
6 D. D. Zhang, J. Feng, H. Wang, Y. F. Liu, L. Chen, Y. Jin, Y. Q. Song, Y. Bai, Q. D. Chen and H. B. Sun, *IEEE Photonics J.*, 2011, **3**, 26.
7 S. R. J. Brueck, in *Proceedings of Institute of Electrical and Electronics Engineers*, New Mexico University, Albuquerque, 2005, pp. 1704–1721.
8 J. Xu, Z. Wang, Z. Weng, Z. Li, X. Sun, L. Liu, L. Zhao, Y. Yue and J. Zhang, *Key Eng. Mater.*, 2013, **552**, 262.
9 N. D. Lai, W. P. Liang, J. H. Lin, C. C. Hsu and C. H. Lin, *Opt. Lett.*, 2005, **13**, 9605.
10 J. H. Moon and S. Yang, *J. Macromol. Sci., Polym. Rev.*, 2005, **45**, 351.
11 J. H. Z. Moon, J. Ford and S. Yang, *Polym. Adv. Technol.*, 2006, **17**, 83.
12 S. Z. Su, A. Rodriguez, S. M. Olaizola, C. S. Peng, C. Tan, Y. K. Verevkin, T. Berthoud and S. Tisserand, *Proc. SPIE*, 2007, **65930**, 1–8.
13 C. G. Chen, R. K. Heilmann, C. Joo, P. T. Konkola, G. S. Pati and M. L. Schattenburg, *J. Vac. Sci. Technol., B: Microelectron. Nanometer Struct.–Process., Meas., Phenom.*, 2002, **20**, 3071.
14 C. P. Fucetola, H. Korre and K. K. Berggren, *J. Vac. Sci. Technol., B: Microelectron. Nanometer Struct.–Process., Meas., Phenom.*, 2009, **27**, 2958.
15 M. Ellman, A. Rodríguez, N. Pérez, M. Echeverria, Y. K. Verevkin, C. S. Peng, T. Berthou, Z. Wang, S. M. Olaizola and I. Ayerdi, *Appl. Surf. Sci.*, 2009, **255**, 5537.
16 W. Zhao, J. Li, H. K. Kang, B. Zhou and C. C. Wong, *Nanosci. Nanotechnol. Lett.*, 2011, **3**, 246.
17 A. F. Lasagni, D. F. Acevedo, C. A. Barbero and F. Mucklich, *Adv. Eng. Mater.*, 2007, **9**, 99.
18 Y. Zabila, M. Perzanowski, A. Dobrowolska, M. Kac, A. Polit and M. Marszalek, *Acta Phys. Pol., A*, 2008, **115**, 591.
19 D. A. Acevedo, A. F. Lasagin, C. A. Barbero and F. Mücklich, *Adv. Mater.*, 2007, **19**, 1272.
20 J. Zhang, Z. Wang, Y. K. Verevkin, S. M. Olaizola, C. Peng, C. Tan, A. Rodriguez, E. Y. Daume, T. Berthou, S. Tisserand and Z. Ji, in *Proc. SPIE 6593, Photonic Materials, Devices, and Applications II*, Maspalomas, Gran Canaria, Spain, 2007, pp. 1–8.
21 C. Tan, C. S. Peng, J. Pakarinen, M. Pessa, V. N. Petryakov, Y. K. Verevkin, J. Zhang, Z. Wang, S. M. Olaizola, T. Berthou and S. Tisserand, *Nanotechnology*, 2009, **20**, 125303.
22 R. Guo, D. Yuan and S. Das, *J. Micromech. Microeng.*, 2011, **21**, 150101.
23 T. Tavera, N. Pérez, A. Rodríguez, P. Yurrita, S. M. Olaizola and E. Castano, *Appl. Surf. Sci.*, 2011, **258**, 1175.
24 D. Wang, Z. Wang, Z. Zhang, Y. Yue, D. Li and C. Maple, *Appl. Surf. Sci.*, 2013, **282**, 67.
25 R. Murillo, H. A. Wolferen, L. Abelmann and J. C. Lodder, *Miner. Eng.*, 2005, **78–79**, 260.
26 L. Wang, B. B. Xu, Q. D. Chen, Z. C. Ma, R. Zhang, Q. X. Liu and H. B. Sun, *Opt. Lett.*, 2011, **36**, 3305.
27 K. M. Baker, *Appl. Opt.*, 1999, **38**, 352.
28 J. Xu, Z. Wang, Z. Zhang, D. Wang and Z. Weng, *J. Appl. Phys.*, 2014, **115**, 203101.

This journal is © The Royal Society of Chemistry 2015